Original Article

Identification of an IFN-β-associated gene signature for the prediction of overall survival among glioblastoma patients

Lijing Cheng[1,2#], Meiling Yuan[1,2#], Shu Li[3], Zhiying Lian[4], Junjing Chen[5], Weibiao Lin[6], Jianbo Zhang[6], Shupeng Zhong[7]

[1]Department of Neurology, The First Affiliated Hospital of Dali University, Dali University, Dali, China; [2]Clinical Medical School, Dali University, Dali, China; [3]Department of Neurology, Jinshan Hospital, Benxi Jinshan Affiliated Hospital of Dalian Medical University, Benxi, China; [4]Second Clinical Medical College, Southern Medical University, Guangzhou, China; [5]Department of Radiation Oncology, Jiangxi Cancer Hospital of Nanchang University, Nanchang, China; [6]Department of Neurosurgery, Zhongshan City People's Hospital, Zhongshan, China; [7]Department of Oncology, Zhongshan City People's Hospital, Zhongshan, China

Contributions: (I) Conception and design: L Cheng, M Yuan; (II) Administrative support: None; (III) Provision of study materials or patients: None; (IV) Collection and assembly of data: J Chen; (V) Data analysis and interpretation: J Zhang, S Li, S Zhong; (VI) Manuscript writing: All authors; (VII) Final approval of manuscript: All authors.

[#]These authors contributed equally to this work.

Correspondence to: Shupeng Zhong. Department of Oncology, Zhongshan City People's Hospital, No. 2 Sunwen Road East, Zhongshan 528403, China. Email: zhongshupeng@163.com; Jianbo Zhang. Department of Neurosurgery, Zhongshan City People's Hospital, No. 2 Sunwen Road East, Zhongshan 528403, China. Email: zjb20191031@163.com.

Background: Brain glioblastoma multiforme (GBM) is the most common primary malignant intracranial tumor. The prognosis of this disease is extremely poor. While the introduction of β-interferon (IFN-β) regimen in the treatment of gliomas has significantly improved the outcome of patients; The mechanism by which IFN-β induces increased TMZ sensitivity has not been described. Therefore, the main objective of the study was to elucidate the molecular mechanisms responsible for the beneficial effect of IFNβ in GBM.

Methods: Messenger RNA expression profiles and clinicopathological data were downloaded from The Cancer Genome Atlas (TCGA) GBM and GSE83300 dataset from the Gene Expression Omnibus. Univariate Cox regression analysis and lasso Cox regression model established a novel 4-gene IFN-β signature (peroxiredoxin 1, Sec61 subunit beta, X-ray repair cross-complementing 5, and Bcl-2-like protein 2) for GBM prognosis prediction. Further, GBM samples (n=50) and normal brain tissues (n=50) were then used for real-time polymerase chain reaction experiments. Gene set enrichment analysis (GSEA) was performed to further understand the underlying molecular mechanisms. Pearson correlation was applied to calculate the correlation between the long non-coding RNAs (lncRNAs) and IFN-β-associated genes. An lncRNA with a correlation coefficient $|R^2|>0.3$ and $P<0.05$ was considered to be an IFN-β-associated lncRNA.

Results: Patients in the high-risk group had significantly poorer survival than patients in the low-risk group. The signature was found to be an independent prognostic factor for GBM survival. Furthermore, GSEA revealed several significantly enriched pathways, which might help explain the underlying mechanisms. Our study identified a novel robust 4-gene IFN-β signature for GBM prognosis prediction. The signature might contain potential biomarkers for metabolic therapy and treatment response prediction for GBM patients.

Conclusions: In the present study, we established a novel IFN-β-associated gene signature to predict the overall survival of GBM patients, which may help in clinical decision making for individual treatment.

Keywords: The Cancer Genome Atlas (TCGA); Gene Expression Omnibus (GEO); Chinese Glioma Genome Atlas (CGGA); β-interferon (IFN-β); glioblastoma; prognostic model

© Annals of Translational Medicine. All rights reserved.

Submitted Mar 29, 2021. Accepted for publication May 06, 2021.
doi: 10.21037/atm-21-1986
View this article at: http://dx.doi.org/10.21037/atm-21-1986

Introduction

Brain glioblastoma multiforme (GBM) is the most common primary malignant intracranial tumor (50%), and is associated with high morbidity and mortality in both adults and children (1-4). A histopathological from low-grade to high-grade transformation is associated with poor overall survival (5). Currently, surgery, radiation, and chemotherapy are the main treatment modalities of GBM. Chemotherapy is a critical process in the postsurgical treatment of GBM (6-8). Alkylating agents, such as temozolomide, remain the standard of care in GBM chemotherapy, but response remains poor (9).

DNA repair protein, O6-methylguanine-DNA methyltransferase (MGMT), plays an essential role in cellular resistance to alkylating agents (10). Clinically, chemoresistance occurs frequently in patients with GBM that exhibit an aberrant activation of MGMT. β-interferon (IFN-β) can act as a drug sensitizer, enhancing toxicity against various neoplasias, and is widely used in combination with other antitumor agents, such as nitrosoureas (11-13). IFN-β sensitizes glioma cells that harbor the unmethylated MGMT promoter and are resistant to temozolomide (11,14,15). Likewise, IFN-β induces loss of spherogenicity and overcomes therapy resistance of glioblastoma stem cells (16). Nevertheless, the specific mechanisms and molecules associated with this phenomenon have not yet been completely elucidated. Therefore, the main objective of the study was to elucidate the molecular mechanisms responsible for the beneficial effect of IFNβ in GBM.

So far, studies have focused mainly on one gene is related with the other. In the present study, we firstly explored and analyzed all differentially expressed IFN-β-associated genes [gene set enrichment analysis (GSEA) M2567] and IFN-β-associated lncRNAs by systematic bioinformatics analysis. In total, 596 GBM patients were included in The Cancer Genome Atlas (TCGA) GBM to construct the prognostic model. Univariate Cox regression model found 5 survival-related genes. Lasso-penalized Cox analysis then identified 5 genes to construct the prognostic model. Using the methodology previously described, the result is validated on the Gene Expression Omnibus (GEO) datasets (GSE83300). We found that a 4 IFN-β-associated gene [peroxiredoxin 1 (*PRDX1*), Sec61 subunit beta (*SEC61B*), X-ray repair cross-complementing 5 (*XRCC5*), and Bcl-2-like protein 2 (*BCL2L2*)] signature was a robust marker of seizure prognosis in patients with GBM. Using data from the Chinese Glioma Genome Atlas (CGGA), we found that 4 IFN-β-associated genes were independent biomarkers of prognosis. Pathway enrichment analysis results demonstrated that several modules are enriched in GBM-related pathways.

Long non-coding RNA (lncRNA) has been demonstrated to play an important role in human diseases (17), especially in GBM. LncRNA AC003092.1 regulates tissue factor pathway inhibitor-2 (TFPI-2) expression through the competing endogenous RNA mechanism, and lncRNA SOX2OT (SOX2 overlapping transcript) interacts with RNA-binding proteins to promote the expression level of SOX2, which is involved in glioma chemotherapy (18,19). However, the relevance between IFN-β and lncRNA has not been fully elucidated in GBM. Pearson correlation was applied to calculate the correlation between lncRNAs and IFN-β-associated genes. An lncRNA with a correlation coefficient $|R^2|>0.3$ and $P<0.05$ was considered to be an IFN-β-associated lncRNA. Univariate and multivariate Cox regressions were used for the survival analysis, which indicated that AC093278.2, AC004067.1, LINC01116, and AC017104.1 were independent prognostic factors for the overall survival of GBM patients.

The findings of the present study may lay the foundation for future studies investigating GBM. We present the following article in accordance with the REMARK reporting checklist (available at http://dx.doi.org/10.21037/atm-21-1986).

Methods

Clinical specimens and data collection

Fifty human glioma tissue samples and 50 normal brain tissues were obtained from the Jiangxi Cancer Hospital of Nanchang University, China. Samples were frozen in liquid nitrogen after surgical resection. All procedures performed in this study involving human participants were in accordance with the Declaration of Helsinki (as revised

© Annals of Translational Medicine. All rights reserved.

in 2013). The present study was approved by the Ethics Committee of the Jiangxi Cancer Hospital of Nanchang University. Informed consent was obtained from patients or guardians.

Messenger RNA (mRNA) expression profiles and clinical data were obtained from TCGA GBM (https://cancergenome.nih.gov/), the GEO (GSE83300) database (https://www.ncbi.nlm.nih.gov/geo/), and the CGGA (http://www.cgga.org.cn/). The IFN-β-associated gene set (M2567) was obtained by GSEA using the gene set database (http://www.gsea-msigdb.org/). All data were analyzed using R software (version 4.0.2) (http://www.r-project.org).

Identification of differentially expressed genes in TCGA GBM

The limma package was used to screen the differentially expressed genes of interest with R software version 4.0.2. The expression pattern of the 120 IFN-β-associated genes was then investigated in TCGA. Genes were selected as consistently altered IFN-β-associated genes for subsequent prognostic analysis if they demonstrated a consistent expression pattern in TCGA cohort and if they were listed in the GSE83300 dataset.

Construction of the prognostic IFN-β-associated gene signature

Univariate Cox regression analysis and lasso-penalized Cox regression analysis were used to identify the prognosis-related IFN-β-associated genes and to construct the prognostic gene signature. $P<0.05$ in the univariate Cox regression analysis was considered statistically significant. The prognostic gene signature was shown as risk score=(coefficient $mRNA_1$×expression of $mRNA_1$)+(coefficient $mRNA_2$×expression of $mRNA_2$)+…+(coefficient mRNAn×expression mRNAn). R package "survival" and "survminer" were used to explore the optimal cut-off of the risk score and to draw the Kaplan-Meier survival curve. In particular, the "surv_cutpoint" function of the "survminer" R package was used to determine the optimal cut-off value to divide patients into the high- and low-risk groups. R package "survivalROC" was used to investigate the time-dependent prognostic value of the gene signature. A 2-sided log-rank $P<0.05$ was considered significant for the survival analysis.

IFN-β-associated lncRNA screening

The profiles of the lncRNAs and IFN-β-associated genes were obtained from TCGA RNAseq dataset. Pearson correlation was applied to calculate the correlation between the lncRNAs and differential genes. An lncRNA with a correlation coefficient $|R^2|>0.3$ and $P<0.05$ was considered to be an IFN-β-associated lncRNA.

Construction of the prognostic IFN-β-associated lncRNA signature

Construction of the prognostic IFN-β-associated lncRNA signature was performed as previously described.

GSEA

GSEA was applied to investigate potential mechanisms underlying the influence of differential gene expression on GBM prognosis. GSEA was also applied to detect whether a priori-defined set of genes showed statistically significant differential expression between the high and low-risk groups. Gene sets with a standard $P<0.05$ were considered to be significantly enriched.

Immunohistochemical staining

The paraffin-embedded glioma tissues were cut into thin slices and then placed on glass slides for the immunohistochemical experiments. The specimens were incubated with rabbit anti-*BCL2L2*, anti-*PRDX1*, anti-*XRCC5*, and *SEC61B* antibody (1:200 dilutions; Abcam, Cambridge, MA, USA) at 4 ℃ overnight, followed by 1-h incubation of biocatalyst secondary antibody (1:200 dilutions, Santa Cruz Biotechnology, Santa Cruz, CA, USA) at room temperature. The avidin-biotin complex method was used to determine the target protein's location and relative expression to visualize the bound antibodies.

Statistical analysis

R 4.0.2 (www.r-project.org/) and SPSS.22 (www.ibm.com/software/it/analytics/spss/) were used to compute statistical analyses. The association between the IFN-β-associated genes and clinicopathologic features was tested using the chi-square test. Comparison of two independent groups was made by two-tailed Students t test. A one-way analysis

© Annals of Translational Medicine. All rights reserved.

of variance (ANOVA) was used to determine differences among groups. Statistical significance was set at *P<0.05, **P<0.01, ***P<0.001. P<0.05 was considered to indicate statistical significance.

Results

Construction and validation of the prognostic IFN-β-associated gene signature

In total, 596 GBM patients and 121 IFN-β-associated genes (70 upregulated and 51 downregulated) were included in TCGA GBM to construct the prognostic model. Differential gene expression analysis identified 14 downregulated and 53 upregulated IFN-β-associated genes, respectively (Table S1). First, the heat map shows the differential genes and analyzed these significant genes further (*Figure 1A*). Univariate Cox regression model found 5 survival-related genes (Table S2). Lasso-penalized Cox analysis identified 5 genes to construct the prognostic model (Table S3). Using the methodology previously described, the result is validated on the GEO datasets (GSE83300) (Table S4). Patients were divided into high- and low-risk groups depending on their risk score. GBM patients with high-risk scores had poor prognosis (*Figure 1B*,*C*). The increased expression of the 4 different signature genes (*PRDX1*, *SEC61B*, *XRCC5*, and *Troxerutin (TXN)* and reduced expression of the 1 signature gene (*BCL2L2*) was observed as the risk value increased (*Figure 1D*,*E*). Taking all of our results together, 4 genes were found to be correlated with unfavorable clinical outcomes.

Prognostic significance of the 4 signature gene expression in GBM

To further validate the expression of the prognostic genes constructing the gene signature, Kaplan-Meier survival analysis was used. The findings indicated that the high expression of *SEC61B* and *XRCC5* was associated with poor prognosis in the GEO dataset (*Figure 2A*,*B*). Moreover, the high expression of SEC61B, *XRCC5*, and *PRDX1* was associated with poor prognosis, and the low expression of *BCL2L2* was associated with poor prognosis in TCGA dataset (*Figure 2C*,*D*,*E*,*F*). To further verify whether the expression of *SEC61B*, *XRCC5*, *BCL2L2*, and *PRDX1* was associated with prognosis in GBM, the Gene Expression Profiling Interactive Analysis (GEPIA) database (https://gepia.cancer-pku.cn/) was used. *SEC61B*, *XRCC5*, and *PRDX1* had significantly high expression in tumor samples compared with normal samples, and *BCL2L2* had significantly low expression in tumor samples compared with normal samples (*Figure 2G*). GBM samples (n=50) and normal brain tissues (n=50) were then used for real-time polymerase chain reaction (PCR) experiments. The results were consistent with the GEPIA database (*Figure 2H*). Taken together, the 4 signature gene expression is considered to be of clinical significance in GBM.

Validation of the 4 signature genes in the CGGA database

To further validate these results, we used the CGGA. Kaplan-Meier survival analysis of the CGGA dataset showed that the high expression of *SEC61B*, *XRCC5*, and *PRDX1*, and the low expression of *BCL2L2* indicated poor patient prognosis (*Figure 3A*,*B*,*C*,*D*). The expression level of *BCL2L2* significantly decreased with higher-grade gliomas (*Figure 3E*). Moreover, the expression of *SEC61B*, *XRCC5*, and *PRDX1* significantly increased with higher-grade gliomas (*Figure 3F*,*G*,*H*). To further validate these results, we performed immunohistochemical experiments. The immunohistochemical results obtained in the present study were consistent with the results of the CGGA database (*Figure 3I*). The expression of the 4 signature genes was considered to be of clinical significance in GBM.

GSEA analysis of the 4 signature genes

To further clarify the impact of the 4 signature genes on GBM, gene ontology and pathway enrichment analyses were performed using GSEA. The results revealed that these genes are mainly enriched in 14 pathways based on TCGA GBM database, including the calcium signaling pathway, cell cycle, epidermal growth factor receptor family (ERBB) signaling pathway, glyceraldehyde-3-phosphate dehydrogenase (GAP) junction, glioma, inositol phosphate metabolism, mitogen-activated protein kinase (MAPK) signaling pathway, oxidative phosphorylation, phosphatidylinositol signaling system, purine metabolism, ribosome, RNA degradation, spliceosome, and vascular endothelial growth factor (VEGR) signaling pathway (*Figure 4A*). Moreover, in the GEO dataset, these genes were mainly enriched in 9 pathways as follows: the calcium signaling pathway, cell cycle, extracellular matrix receptor interaction, ERBB signaling pathway, inositol phosphate metabolism, oxidative phosphorylation, P53 signaling pathway, phosphatidylinositol signaling system,

© Annals of Translational Medicine. All rights reserved.

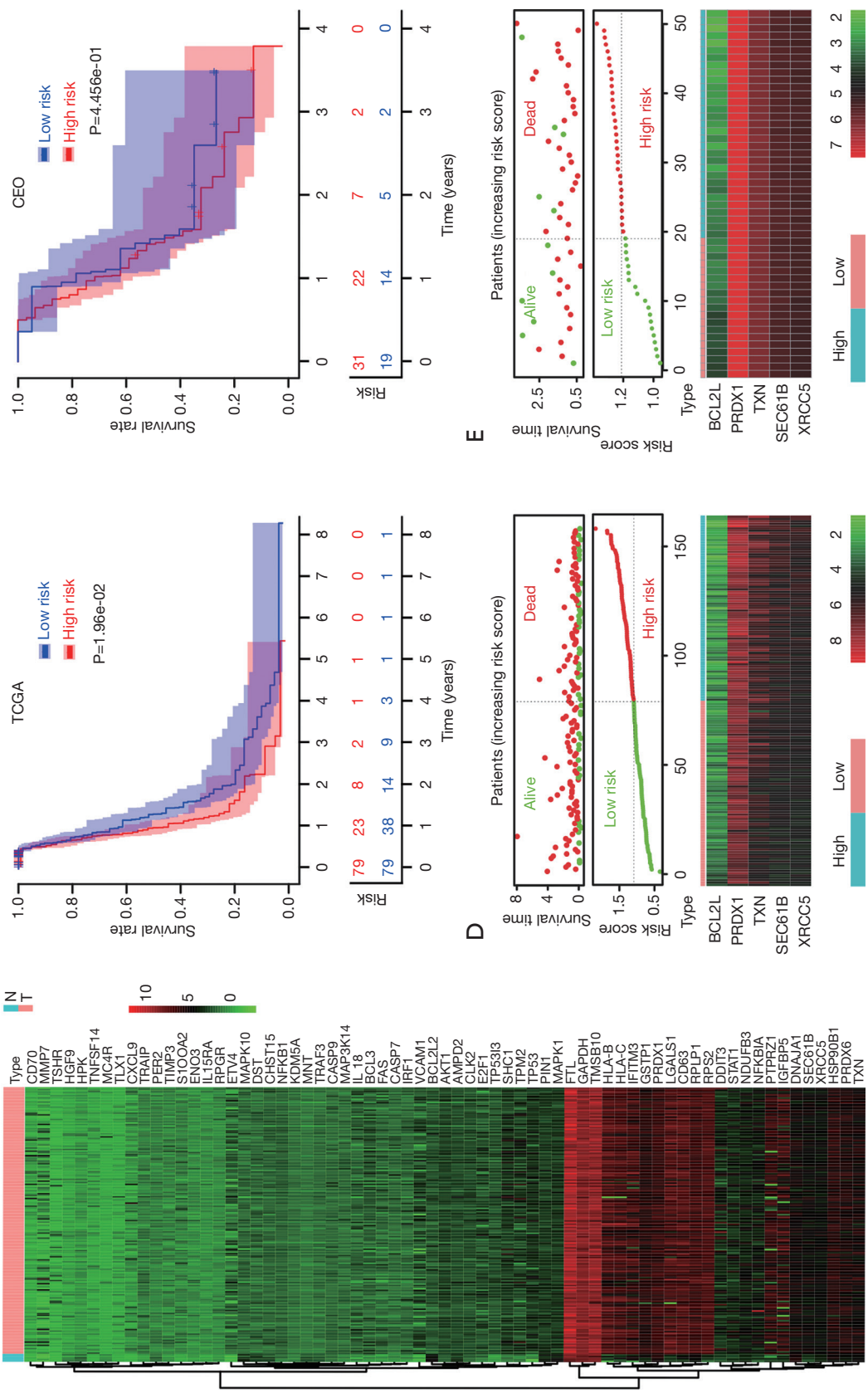

Figure 1 Construction and validation of the prognostic β-interferon (IFN-β)-associated genes signature. (A) Heatmap showing differential expression of 67 genes in normal brain tissues and glioblastoma multiforme (GBM) tissues, which differed significantly ($P<0.05$). (B) Survival curve of GBM patients based on risk score model in The Cancer Genome Atlas (TCGA). (C) Survival curve of GBM patients based on risk score model in TCGA. (D,E) Survival duration and status of GBM cases. IFN-β-associated gene risk score analysis of GBM patients in TCGA and the Gene Expression Omnibus (GEO). Heatmap of the 5 key genes expressed in GBM.

© Annals of Translational Medicine. All rights reserved.

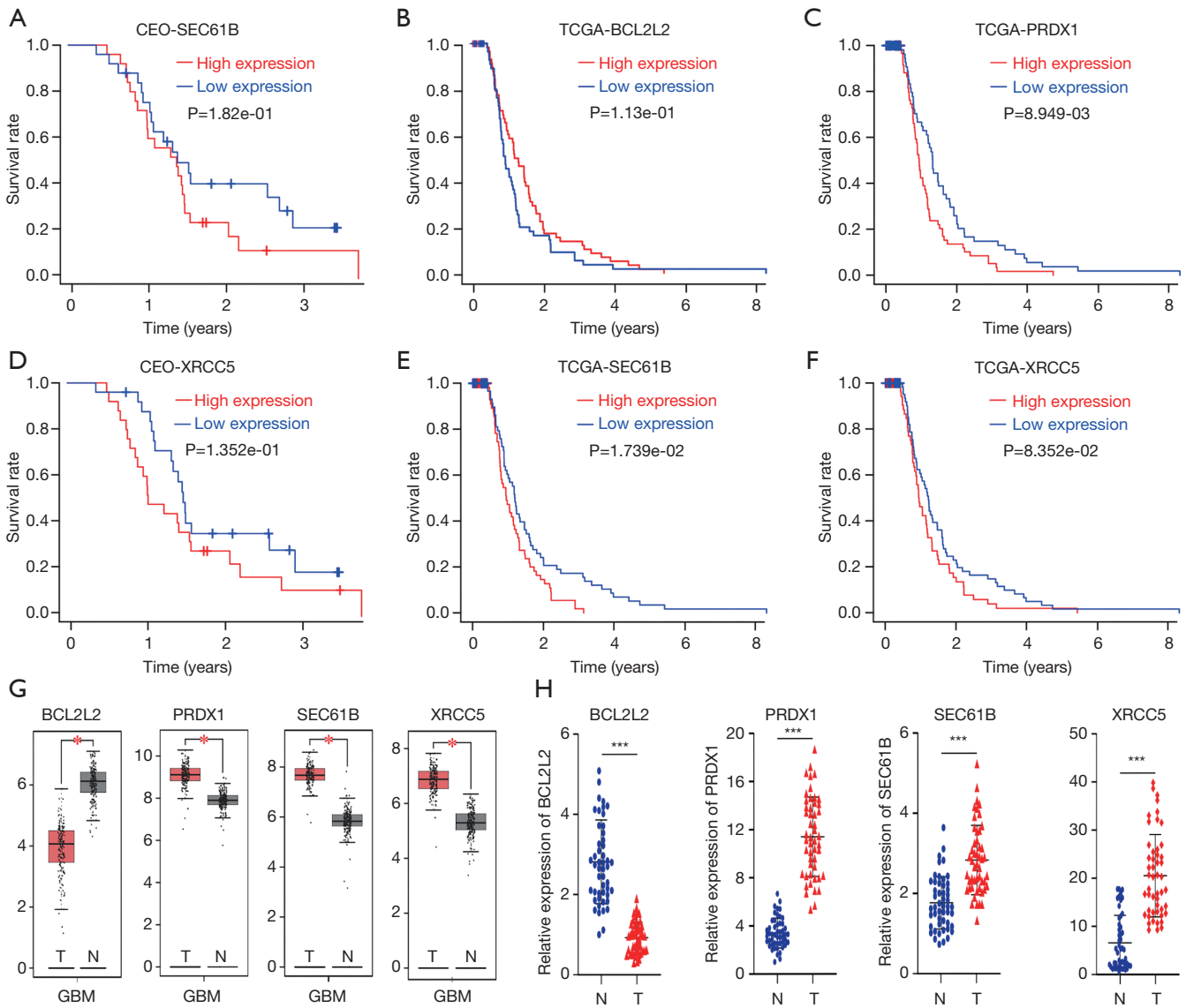

Figure 2 Prognostic significance of 4 signature gene expression in glioblastoma multiforme (GBM). (A,B) Survival analysis of the 2 prognostic β-interferon (IFN-β)-associated genes based on the Gene Expression Omnibus (GEO) database. (C,D,E,F) Survival analysis of the 4 prognostic IFN-β-associated genes based on The Cancer Genome Atlas (TCGA) database. (G) Expression analysis of 4 prognostic IFN-β-associated genes according to the Gene Expression Profiling Interactive Analysis database. (H) Real-time polymerase expression analysis of 4 prognostic IFN-β-associated genes in normal brain tissues (n=50) and GBM tissues (n=50). *P<0.05, ***P<0.001.

and pyrimidine metabolism (*Figure 4B*). These genes may be involved in the proliferation of GBM.

Prognostic impact of IFN-β-associated lncRNA signature for GBM

Considering the critical role of lncRNAs in GBM, the identification of important lncRNAs in cancer and developing lncRNA-based therapeutic strategies are important. Pearson correlation was applied to calculate the correlation between lncRNAs and IFN-β-associated genes. An lncRNA with a correlation coefficient $|R^2|>0.3$ and P<0.05 was considered to be an IFN-β-associated lncRNA. Univariate and multivariate Cox regressions were used for the survival analysis, and indicated that AC093278.2, AC004067.1, LINC01116, and AC017104.1

© Annals of Translational Medicine. All rights reserved.

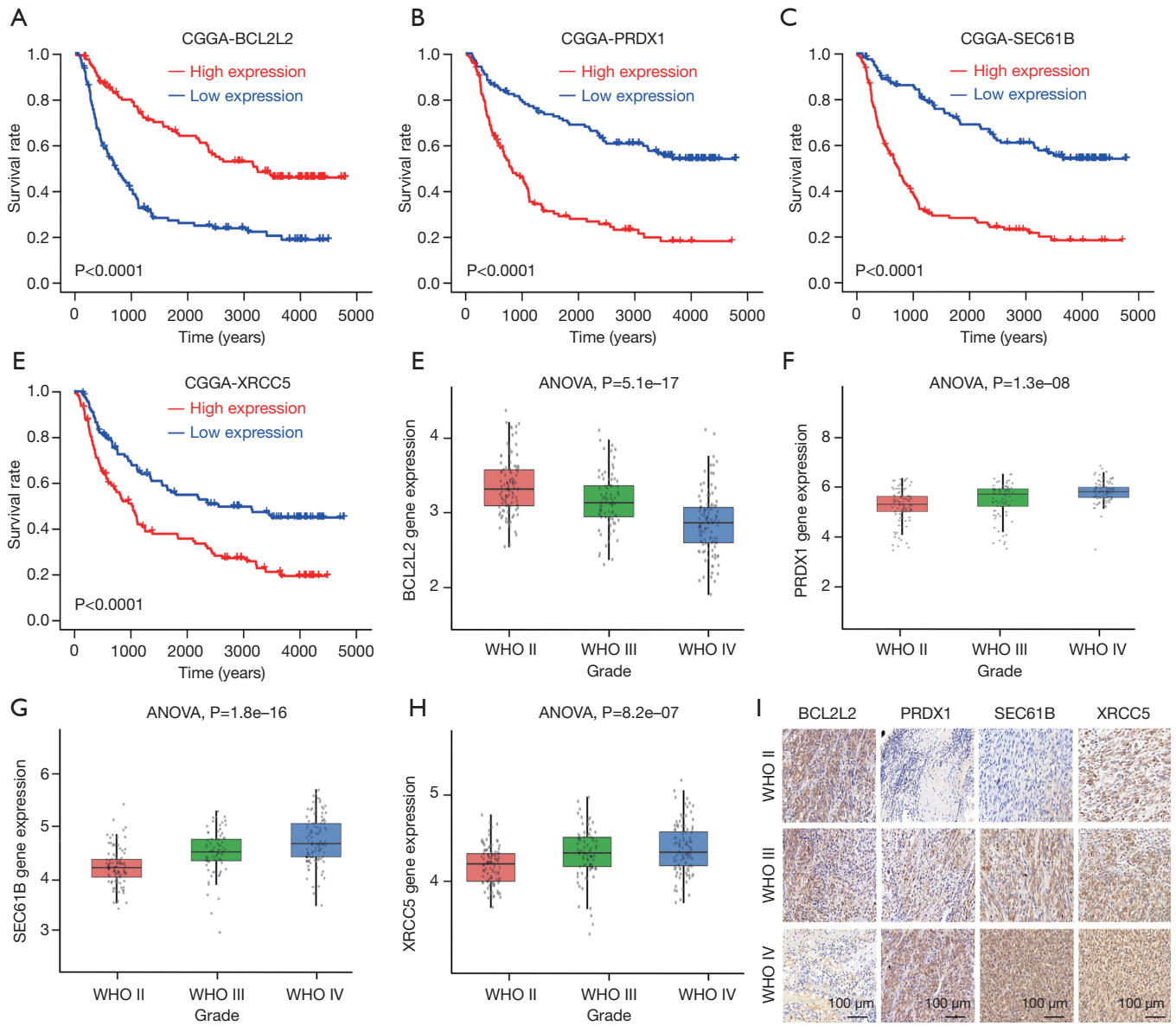

Figure 3 Validation of four signature-genes in the Chinese Glioma Genome Atlas (CGGA) database. (A,B,C,D) Survival analysis of the 4 prognostic β-interferon (IFN-β)-associated genes based on the CGGA database. (E,F,G,H) Expression analysis of 4 prognostic IFN-β-associated genes according to the CGGA database. (I) Immunohistochemistry of the 4 prognostic IFN-β-associated genes.

were independent prognostic factors for the overall survival of GBM patients (*Figure 5A,B,C*). Moreover, the high expression of the AC004067.1, AC017104.1, and LINC01116 is associated with poor prognosis, and the low expression of AC093278.2 is associated with poor prognosis in TCGA dataset (*Figure 5D,E,F,G*). GBM samples (n=50) and normal brain tissues (n=50) were then used for real-time PCR experiments to validate the expression of the IFN-β-associated lncRNAs in GBM. RT-PCR showed that, compared with the normal brain tissues, AC004067.1, AC017104.1, and LINC01116 were highly expressed and AC093278.2 and a low expression in GBM (*Figure 5H*). Therefore, IFN-β-associated lncRNAs have a high diagnostic value for GBM.

Discussion

With the development of high-throughput sequencing

© Annals of Translational Medicine. All rights reserved.

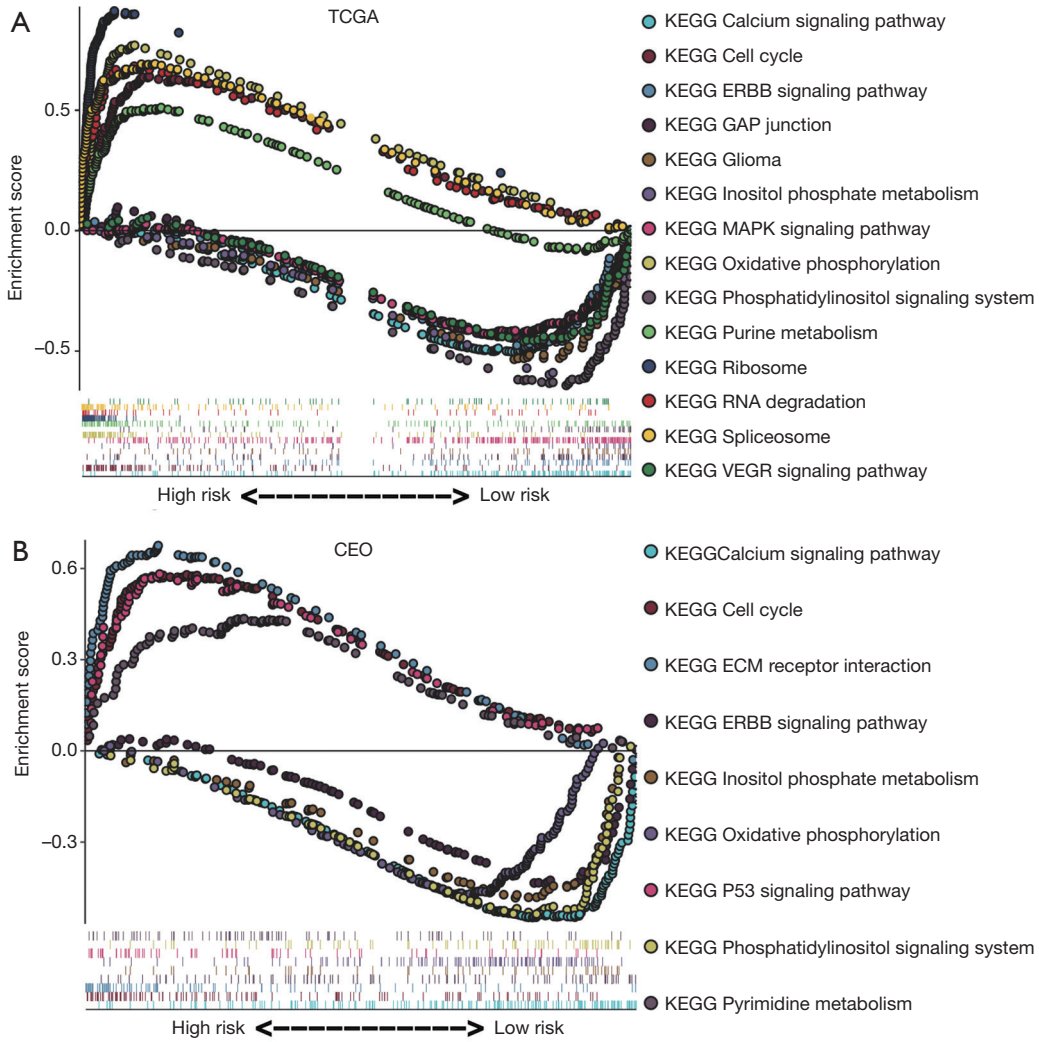

Figure 4 Gene set enrichment analysis (GSEA) analysis of the 4 signature genes. (A,B) GSEA analysis of the 4 prognostic β-interferon (IFN-β)-associated genes based on The Cancer Genome Atlas (TCGA) and the Gene Expression Omnibus (GEO) database.

technology, the understanding of cancer is becoming clearer. As the scope of analyzed genes and diseases expands, bioinformatics analysis is becoming increasingly important. In the present study, we analyzed the biological functions of a prognostic IFN-β-associated gene signature using bioinformatics analysis.

Univariate Cox regression model found 5 survival-related genes. Lasso-penalized Cox analysis identified 5 genes to construct the prognostic model. Using the methodology previously described, the result is validated on the GEO datasets (GSE83300). We found that 4 IFN-β-associated genes (*PRDX1*, *SEC61B*, *XRCC5*, and *BCL2L2*) signature was a suitable marker of seizure prognosis in patients with GBM. Using the CGGA data, we found that 4 IFN-β-associated genes are independent biomarkers of prognosis and play important roles in many biological processes. For example, *PRDX1* is a member of the peroxiredoxin family of antioxidant enzymes, which reduce hydrogen peroxide and alkyl hydroperoxides (20). *PRDX1* forms a heterodimer with p38α MAPK14, stabilizing phosphate-p38α in glioma cells (21), and epigenetic silencing of *PRDX1* is frequent in 1p/19q-deleted oligodendroglial tumors and likely contributes to radiosensitivity and chemosensitivity of these tumors (22). *XRCC5* is the 80-kD subunit of the Ku heterodimer protein, which is also known as ATP-dependent DNA helicase II or DNA repair protein *XRCC5*.

© Annals of Translational Medicine. All rights reserved.

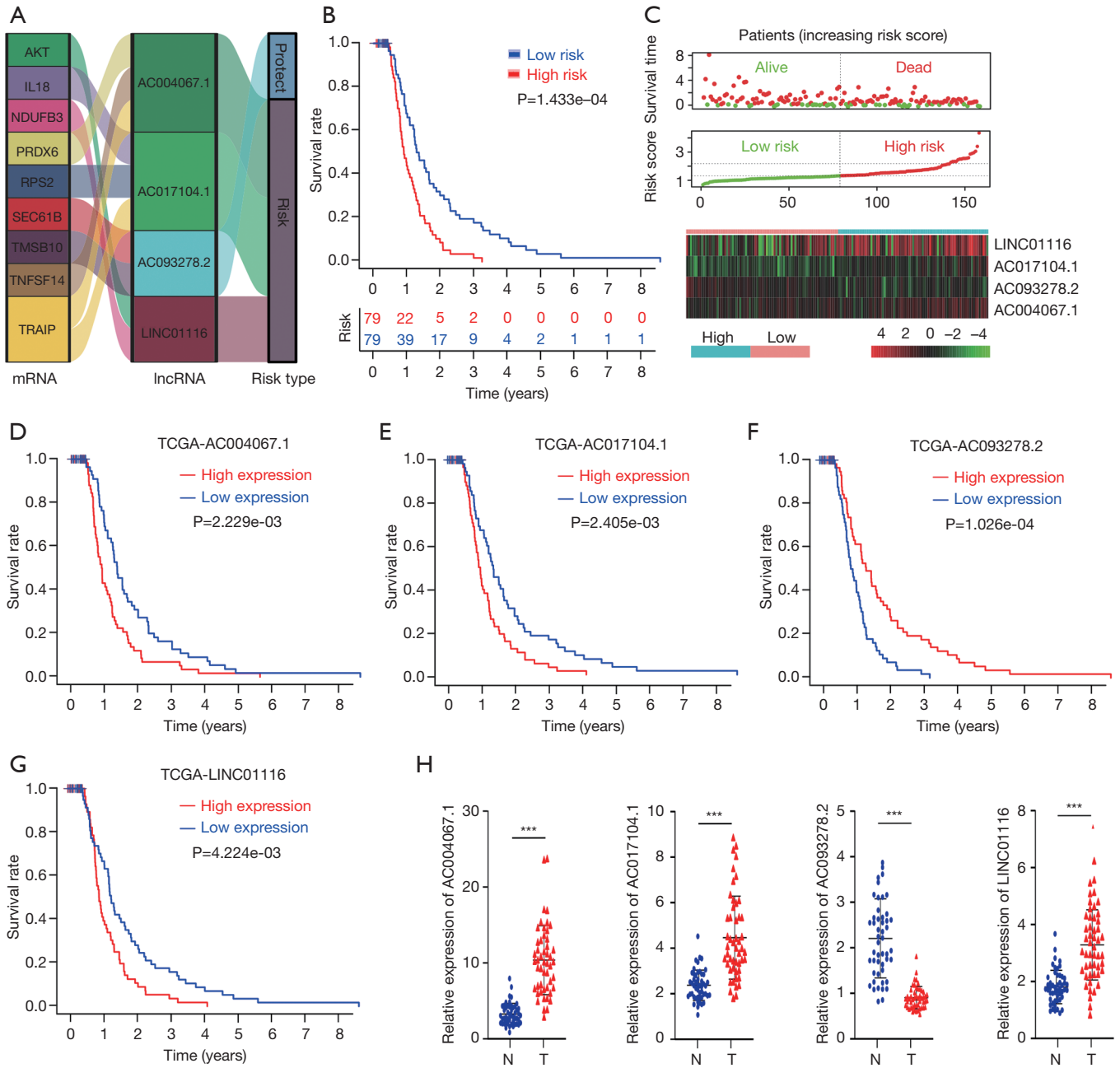

Figure 5 Prognostic impact of the β-interferon (IFN-β)-associated lncRNA signature for glioblastoma multiforme (GBM). (A) Network of prognostic lncRNAs with co-expressed IFN-β-associated lncRNAs in GBM. (B) Survival curve of GBM patients based on risk score model in The Cancer Genome Atlas (TCGA). (C) Survival duration and status of GBM cases. IFN-β-associated lncRNA risk score analysis of GBM patients in TCGA. Heatmap of the 4 key lncRNAs expressed in GBM. (D,E,F,G) Survival analysis of the 4 prognostic IFN-β-associated lncRNAs based on TCGA database. (H) Real-time polymerase chain reaction expression analysis of 4 prognostic IFN-β-associated lncRNAs in normal brain tissues (n=50) and GBM tissues (n=50). ***P<0.001.

© Annals of Translational Medicine. All rights reserved.

The polymorphisms of *XRCC5* play an important role in astrocytoma prognosis in the Chinese Han population, which could be used in the determination of astrocytoma prognosis in clinical research (23). Elevated XRCC5 expression level can promote temozolomide resistance and predict poor prognosis in glioblastoma (24). *BCL2L2* is a member of the Bcl-2 protein family. The proteins of this family form heterodimers or homodimers and act as anti- and pro-apoptotic regulators. The expression of (24) in various cancer cell types. Interestingly, *BCL2L2* mRNA is highly expressed in the mesenchymal type of GBM (25). Through the wide variety of studies published to date, no clear consensus for the BCL2L2 is correlated with radiotherapy and chemotherapy in GBM. *SEC61B* is the central component of the protein translocation apparatus of the endoplasmic reticulum membrane (26). However, to the best of our knowledge, the expression pattern and function of SEC61B in GBM have not been previously reported; the role of the BCL2L2, XRCC5, SEC61B in glioma radiotherapy still remains unclear. Therefore, further study is warranted.

Considering the critical role of lncRNAs in GBM, the identification of important lncRNAs in cancer and developing lncRNA-based therapeutic strategies will be important in the future. Univariate and multivariate Cox Pearson correlation was applied to calculate the correlation between the lncRNAs and IFN-β-associated genes. regressions were used for the survival analysis, and indicated that AC093278.2, AC004067.1, LINC01116, and AC017104.1 were independent prognostic factors for the overall survival of GBM patients. LncRNA genes play important roles in many biological processes. For example, LINC01116 promotes tumor proliferation, migration, and invasion in glioma cell (27,28). However, the role of AC093278.2, AC004067.1, and AC017104.1 in GBM has not been reported, and it is important that it is elucidated in future studies. All in all, a novel IFN-β-associated gene signature to predict the overall survival of GBM patients, which may help in clinical decision making for individual treatment.

Conclusions

In the present study, we explored and analyzed differentially expressed IFN-β-associated genes by systematic bioinformatics analysis and established a novel IFN-β-associated gene signature to predict the overall survival of GBM patients, which may help in clinical decision making for individual treatment.

Acknowledgments

We are very grateful to all of the participants in the present research and the highly valuable comments of Zhou Jian. We also thank the reviewers for their valuable advice.
Funding: None.

Footnote

Reporting Checklist: The authors have completed the REMARK reporting checklist. Available at http://dx.doi.org/10.21037/atm-21-1986

Data Sharing Statement: Available at http://dx.doi.org/10.21037/atm-21-1986

Conflicts of Interest: All authors have completed the ICMJE uniform disclosure form (available at http://dx.doi.org/10.21037/atm-21-1986). The authors have no conflicts of interest to declare.

Ethical Statement: The authors are accountable for all aspects of the work in ensuring that questions related to the accuracy or integrity of any part of the work are appropriately investigated and resolved. All procedures performed in this study involving human participants were in accordance with the Declaration of Helsinki (as revised in 2013). The study was approved by the Ethics Committee of the Jiangxi Cancer Hospital of Nanchang University. Informed consent was obtained from the patients or guardians.

Open Access Statement: This is an Open Access article distributed in accordance with the Creative Commons Attribution-NonCommercial-NoDerivs 4.0 International License (CC BY-NC-ND 4.0), which permits the non-commercial replication and distribution of the article with the strict proviso that no changes or edits are made and the original work is properly cited (including links to both the formal publication through the relevant DOI and the license). See: https://creativecommons.org/licenses/by-nc-nd/4.0/.

References

1. Alexander BM, Ba S, Berger MS, et al. Adaptive Global Innovative Learning Environment for Glioblastoma: GBM

© Annals of Translational Medicine. All rights reserved.

AGILE. Clin Cancer Res 2018;24:737-43.
2. Louis DN, Ohgaki H, Wiestler OD, et al. The 2007 WHO classification of tumours of the central nervous system. Acta Neuropathol 2007;114:97-109.
3. Majc B, Novak M, Jerala NK, et al. Immunotherapy of Glioblastoma: Current Strategies and Challenges in Tumor Model Development. Cells 2021;10:265.
4. Oronsky B, Reid TR, Oronsky A, et al. A Review of Newly Diagnosed Glioblastoma. Front Oncol 2021;10:574012.
5. Ho AL, Koch MJ, Tanaka S, et al. Impact of histopathological transformation and overall survival in patients with progressive anaplastic glioma. J Clin Neurosci 2016;31:99-105.
6. Weller M, van den Bent M, Hopkins K, et al. EANO guideline for the diagnosis and treatment of anaplastic gliomas and glioblastoma. Lancet Oncol 2014;15:e395-403.
7. Uddin MS, Mamun AA, Alghamdi BS, et al. Epigenetics of glioblastoma multiforme: From molecular mechanisms to therapeutic approaches. Semin Cancer Biol 2020:S1044-579X(20)30275-3.
8. Sulman EP, Ismaila N, Armstrong TS, et al. Radiation Therapy for Glioblastoma: American Society of Clinical Oncology Clinical Practice Guideline Endorsement of the American Society for Radiation Oncology Guideline. J Clin Oncol 2017;35:361-9.
9. Azam Z, To ST, Tannous BA. Mesenchymal Transformation: The Rosetta Stone of Glioblastoma Pathogenesis and Therapy Resistance. Adv Sci (Weinh) 2020;7:2002015.
10. Peng Y, Pei H. DNA alkylation lesion repair: outcomes and implications in cancer chemotherapy. J Zhejiang Univ Sci B 2021;22:47-62.
11. Ochiai Y, Sumi K, Sano E, et al. Antitumor effects of ribavirin in combination with TMZ and IFN-beta in malignant glioma cells. Oncol Lett 2020;20:178.
12. GuhaSarkar D, Su Q, Gao G, et al. Systemic AAV9-IFNbeta gene delivery treats highly invasive glioblastoma. Neuro Oncol 2016;18:1508-18.
13. Hong YK, Chung DS, Joe YA, et al. Efficient inhibition of in vivo human malignant glioma growth and angiogenesis by interferon-beta treatment at early stage of tumor development. Clin Cancer Res 2000;6:3354-60.
14. Natsume A, Aoki K, Ohka F, et al. Genetic analysis in patients with newly diagnosed glioblastomas treated with interferon-beta plus temozolomide in comparison with temozolomide alone. J Neurooncol 2020;148:17-27.
15. Makita K, Hara H, Sano E, et al. Interferon-beta sensitizes human malignant melanoma cells to temozolomide-induced apoptosis and autophagy. Int J Oncol 2019;54:1864-74.
16. Happold C, Roth P, Silginer M, et al. Interferon-beta induces loss of spherogenicity and overcomes therapy resistance of glioblastoma stem cells. Mol Cancer Ther 2014;13:948-61.
17. Statello L, Guo CJ, Chen LL, et al. Gene regulation by long non-coding RNAs and its biological functions. Nat Rev Mol Cell Biol 2021;22:96-118.
18. Liu B, Zhou J, Wang C, et al. LncRNA SOX2OT promotes temozolomide resistance by elevating SOX2 expression via ALKBH5-mediated epigenetic regulation in glioblastoma. Cell Death Dis 2020;11:384.
19. Xu N, Liu B, Lian C, et al. Long noncoding RNA AC003092.1 promotes temozolomide chemosensitivity through miR-195/TFPI-2 signaling modulation in glioblastoma. Cell Death Dis 2018;9:1139.
20. Kisucka J, Chauhan AK, Patten IS, et al. Peroxiredoxin1 prevents excessive endothelial activation and early atherosclerosis. Circ Res 2008;103:598-605.
21. Wirthschaft P, Bode J, Simon AEM, et al. A PRDX1-p38alpha heterodimer amplifies MET-driven invasion of IDH-wildtype and IDH-mutant gliomas. Int J Cancer 2018;143:1176-87.
22. Dittmann LM, Danner A, Gronych J, et al. Downregulation of PRDX1 by promoter hypermethylation is frequent in 1p/19q-deleted oligodendroglial tumours and increases radio- and chemosensitivity of Hs683 glioma cells in vitro. Oncogene 2012;31:3409-18.
23. He X, Zhu X, Li L, et al. The relationship between polymorphisms of XRCC5 genes with astrocytoma prognosis in the Han Chinese population. Oncotarget 2016;7:85283-90.
24. Lee IN, Yang JT, Huang C, et al. Elevated XRCC5 expression level can promote temozolomide resistance and predict poor prognosis in glioblastoma. Oncol Lett 2021;21:443.
25. Chung HJ, Choi YE, Kim ES, et al. miR-29b attenuates tumorigenicity and stemness maintenance in human glioblastoma multiforme by directly targeting BCL2L2. Oncotarget 2015;6:18429-44.
26. Zhu Y, Zhang G, Lin S, et al. Sec61beta facilitates the maintenance of endoplasmic reticulum homeostasis by associating microtubules. Protein Cell 2018;9:616-28.
27. Wang T, Cao L, Dong X, et al. LINC01116 promotes tumor proliferation and neutrophil recruitment via DDX5-mediated regulation of IL-1beta in glioma cell. Cell Death Dis 2020;11:302.

© Annals of Translational Medicine. All rights reserved.

28. Zhang N, Shuai K, Cheng J, et al. LncRNA linc01116 prometes glioma cell migration and invasion by modulation of radixin targeted by miR-31. Int J Clin Exp Pathol 2019;12:1078-86.

(English Language Editor: R. Scott)

Cite this article as: Cheng L, Yuan M, Li S, Lian Z, Chen J, Lin W, Zhang J, Zhong S. Identification of an IFN-β-associated gene signature for the prediction of overall survival among glioblastoma patients. Ann Transl Med 2021;9(11):925. doi: 10.21037/atm-21-1986

© Annals of Translational Medicine. All rights reserved.

Table S1 Differential gene expression analysis identified 14 downregulated and 53 upregulated IFN-β-associated genes.

gene	conMean	treatMean	logFC	pValue	fdr
CD63	30.10657	313.0741	3.378354	0.000172	0.002036
CD70	0.555679	2.200962	1.98581	0.000832	0.002797
E2F1	3.505146	10.48335	1.580554	0.007463	0.013579
FTL	651.6117	3210.001	2.300489	0.000599	0.002369
GAPDH	512.1522	1157.601	1.176493	0.001146	0.00318
GSTP1	32.61208	108.6335	1.735991	0.000337	0.002036
LGALS1	17.39993	328.6125	4.239234	0.000206	0.002036
MNT	6.166503	3.011482	-1.03398	0.000325	0.002036
NDUFB3	20.31884	32.20039	0.66426	0.021104	0.033464
NFKBIA	10.93926	56.22313	2.361648	0.000779	0.002703
PIN1	27.5438	14.49285	-0.92639	0.001473	0.003803
PRDX1	83.12447	162.8397	0.970107	0.00152	0.003833
PRDX6	34.97637	82.92948	1.245504	0.000619	0.002369
RPLP1	42.436	203.9833	2.26509	0.000149	0.002036
RPS2	14.01768	276.6118	4.302543	0.000144	0.002036
S100A2	0.755174	2.902967	1.942647	0.000237	0.002036
SEC61B	12.62775	46.94838	1.894478	0.000144	0.002036
SHC1	3.090129	19.56899	2.66283	0.000206	0.002036
TMSB10	662.5164	1667.381	1.331555	0.003943	0.007816
TP53I3	1.08063	8.602309	2.992851	0.000144	0.002036
TPM2	3.217674	18.44204	2.518909	0.000916	0.002906
TRAF3	5.798808	3.876128	-0.58114	0.002193	0.00507
TSHR	0.52064	1.21914	1.227504	0.008086	0.014477
TXN	42.52225	70.3807	0.726962	0.01964	0.031595
XRCC5	24.69804	41.33577	0.742994	0.000373	0.002072
AKT1	5.828089	11.30404	0.955743	0.001341	0.003545
AMPD2	17.22854	9.199601	-0.90516	0.007264	0.013439
BCL2L2	41.065	8.016368	-2.35689	0.000144	0.002036
BCL3	1.536024	7.403995	2.269103	0.000507	0.002369
CASP7	1.701272	4.602387	1.435769	0.000428	0.002262
CASP9	3.27981	4.734607	0.529632	0.022131	0.034119
CHST15	7.984939	5.270313	-0.59939	0.025479	0.038742
CLK2	5.013503	9.431446	0.91166	0.002328	0.005274
CXCL9	0.522583	2.959908	2.50182	0.000303	0.002036
DDIT3	10.53898	39.86037	1.91922	0.004295	0.008364
DNAJA1	81.49636	57.45116	-0.5044	0.016566	0.027444
DST	11.587	4.898513	-1.24209	0.000619	0.002369
ENO3	1.078342	1.936191	0.844407	0.002866	0.006118
ETV4	0.449016	5.842307	3.7017	0.000524	0.002369
FAS	1.211993	5.397376	2.154877	0.000619	0.002369
FGF9	2.489786	1.05976	-1.23228	0.002193	0.00507
HLA-B	13.25433	323.677	4.610019	0.000185	0.002036
HLA-C	21.08252	260.7631	3.62862	0.000214	0.002036
HRK	4.302541	1.496812	-1.5233	0.000887	0.002896
HSP90B1	53.99334	105.0129	0.959713	0.002193	0.00507
IFITM3	37.89578	210.6592	2.474802	0.001146	0.00318
IGFBP5	15.80209	156.8898	3.311564	0.001075	0.00318
IL15RA	0.909774	1.710014	0.910427	0.000337	0.002036
IL18	1.533749	6.167387	2.007597	0.00111	0.00318
IRF1	1.646495	5.161978	1.648526	0.001146	0.00318
KDM5A	2.286764	3.631279	0.66717	0.001943	0.004792
MAP3K14	1.968346	4.329348	1.137166	0.000348	0.002036
MAPK1	37.5546	15.92404	-1.23778	0.00126	0.003411
MAPK10	16.65285	4.83445	-1.78434	0.000683	0.002529
MC4R	1.741701	0.887979	-0.9719	0.000328	0.002036
MMP7	0.39799	4.360563	3.453711	0.003039	0.006247
NFKB1	3.08316	5.389852	0.805836	0.002546	0.005653
PER2	4.063261	2.574965	-0.65809	0.006518	0.012263
PTPRZ1	9.053498	136.0179	3.909177	0.000542	0.002369
RPGR	1.267263	2.035992	0.684016	0.002952	0.006181
STAT1	11.88487	29.58109	1.315548	0.002866	0.006118
TIMP3	1.351658	2.491341	0.882192	0.014275	0.024759
TLX1	0.606327	1.01475	0.742957	0.000764	0.002703
TNFSF14	0.682826	1.188035	0.798987	0.003129	0.006316
TP53	1.339876	18.70788	3.803475	0.000179	0.002036
TRAIP	1.100777	2.933994	1.414344	0.000314	0.002036
VCAM1	0.722361	10.0756	3.802003	0.000619	0.002369

Table S2 Univariate Cox regression model found 5 survival-related genes

id	HR	HR.95L	HR.95H	pvalue
PRDX1	1.002986	1.000224	1.005755	0.034085
SEC61B	1.018342	1.005051	1.03181	0.006698
TXN	1.007272	1.000557	1.014032	0.03375
XRCC5	1.025477	1.005747	1.045595	0.011145
BCL2L2	0.944842	0.894724	0.997768	0.041319

© Annals of Translational Medicine. All rights reserved.
http://dx.doi.org/10.21037/atm-21-1986

Table S3 Lasso-penalized Cox analysis identified 5 genes to construct the prognostic model

id	futime	fustat	PRDX1	SEC61B	TXN	XRCC5	BCL2L2	riskScore	risk
TCGA-19-5960	0.013699	0	140.3251	29.66717	42.88298	69.56536	8.375261	1.564664	high
TCGA-06-5418	0.019178	0	118.8639	39.67598	64.92846	33.20539	12.76465	0.848628	low
TCGA-12-1597	0.054795	0	142.8102	49.3957	51.56646	40.8878	6.976729	1.180437	high
TCGA-32-4213	0.071233	0	138.0042	40.21844	32.29656	40.58741	5.224391	1.129728	low
TCGA-14-0871	0.076712	0	98.02954	84.35446	76.9631	69.41546	6.750546	1.831538	high
TCGA-14-0790	0.093151	0	173.3056	56.72675	67.44097	35.26562	3.706071	1.260257	high
TCGA-32-2616	0.123288	0	136.5546	37.67904	84.84546	41.9269	7.657441	1.167249	low
TCGA-28-2509	0.128767	0	167.6415	46.34816	100.2417	33.30769	5.840747	1.168708	low
TCGA-06-2558	0.134247	0	206.7004	54.56901	64.06912	50.17674	9.021406	1.468887	high
TCGA-27-1831	0.147945	0	224.5134	85.01386	76.92627	30.65479	1.804257	1.459245	high
TCGA-19-4065	0.156164	0	111.5957	80.26543	175.2979	37.46402	16.77551	1.189536	high
TCGA-76-4928	0.186301	0	126.2451	59.36295	101.6404	43.99712	7.968783	1.308979	high
TCGA-02-2483	0.224658	0	103.1318	78.0226	221.6511	82.41142	6.414456	2.271565	high
TCGA-06-2565	0.257534	0	134.3475	34.55243	41.9556	39.66919	9.606255	1.002286	low
TCGA-06-0221	0.263014	0	109.8401	20.9592	35.09466	45.88823	22.92124	0.718923	low
TCGA-19-2620	0.268493	0	171.5653	34.255	45.71353	24.66921	13.49417	0.719022	low
TCGA-06-0188	0.268493	0	157.493	41.18219	81.36895	60.2722	11.21148	1.479606	high
TCGA-28-5208	0.271233	0	233.758	52.12235	82.99764	57.8433	7.005562	1.717449	high
TCGA-19-1787	0.273973	0	134.0508	38.18114	62.76541	51.43739	5.878342	1.343401	high
TCGA-06-5412	0.279452	0	158.7072	41.60444	49.7972	36.22516	9.70667	1.027343	low
TCGA-19-1389	0.284932	0	143.523	45.00921	147.8676	42.3617	8.237626	1.305182	high
TCGA-26-5134	0.287671	0	143.8337	71.34361	87.63025	42.11121	4.609562	1.41316	high
TCGA-06-2561	0.30137	0	129.4165	26.95697	27.06816	35.69237	9.664078	0.860468	low
TCGA-06-0174	0.309589	0	135.2137	42.86477	42.50185	55.87772	5.421822	1.428654	high
TCGA-27-2524	0.312329	0	154.5816	100.9761	166.88	43.40007	6.635765	1.674917	high
TCGA-32-5222	0.315068	0	249.77	52.27965	88.19906	50.01179	4.78742	1.657946	high
TCGA-41-5651	0.326027	0	152.466	40.48911	116.6978	60.24457	10.65221	1.530896	high
TCGA-06-0158	0.331507	0	120.1098	32.92711	39.32712	32.09478	10.14526	0.814416	low
TCGA-06-0138	0.345205	0	152.6425	54.89752	85.10129	28.5542	2.827759	1.135179	low
TCGA-14-2554	0.347945	0	168.2275	63.95563	73.87036	35.23214	5.07638	1.266138	high
TCGA-28-5204	0.350685	0	127.6719	28.99288	71.11637	44.76476	9.008068	1.112678	low
TCGA-19-1390	0.356164	0	48.07005	36.19385	27.43887	37.05623	5.534106	0.866978	low
TCGA-06-0646	0.364384	0	99.09356	35.56775	46.89974	43.21746	4.947798	1.11174	low
TCGA-12-0618	0.364384	0	67.443	54.4239	120.9357	59.02999	9.576032	1.448237	high
TCGA-28-5209	0.369863	0	229.5587	38.23931	69.0032	45.6831	7.450065	1.390104	high
TCGA-26-5136	0.372603	0	192.7499	71.43491	108.2516	49.15737	12.54333	1.498292	high
TCGA-12-5295	0.389041	0	301.1052	63.88231	125.8404	46.04834	2.670659	1.835403	high
TCGA-32-1970	0.394521	0	108.0138	22.59641	25.95279	37.36755	9.544778	0.831774	low
TCGA-28-2499	0.39726	0	287.5934	24.36353	31.9343	35.21199	3.168737	1.271774	high
TCGA-02-2485	0.4	0	122.7897	37.32248	42.40419	64.6278	6.116927	1.525002	high
TCGA-06-5413	0.4	0	235.1694	60.04048	59.99449	60.03172	5.626302	1.792517	high
TCGA-06-0139	0.405479	0	180.1379	62.03357	101.702	28.21095	3.903835	1.216003	high
TCGA-06-0744	0.413699	0	142.3851	54.56737	29.33902	31.89612	7.657043	0.992391	low
TCGA-06-5411	0.419178	0	174.0267	48.40504	97.56886	39.33645	16.05117	1.084493	low
TCGA-06-0686	0.421918	0	193.3583	52.96145	57.03175	39.39186	7.497999	1.260213	high
TCGA-06-0129	0.430137	1	64.39262	28.57973	30.56102	47.85222	9.750011	0.975217	low
TCGA-06-2567	0.438356	1	171.171	34.98164	61.42383	57.83904	6.989487	1.488365	high
TCGA-06-5408	0.452055	1	180.6637	52.13031	74.65464	54.80463	5.087023	1.591817	high
TCGA-76-4927	0.487671	1	195.3624	54.4249	56.66848	39.63224	9.78166	1.227297	high
TCGA-06-0878	0.487671	1	195.2847	50.80717	92.53551	49.44408	5.464186	1.532894	high
TCGA-06-0644	0.490411	1	176.7468	77.41673	173.0849	52.90885	4.969178	1.820638	high
TCGA-14-0789	0.512329	1	85.53151	30.52127	53.45421	32.2351	9.854335	0.769117	low
TCGA-27-1837	0.512329	1	170.7995	39.68927	45.59562	28.03151	8.16817	0.915896	low
TCGA-12-5299	0.517808	1	201.5399	71.76869	99.38701	43.24753	5.812191	1.53445	high
TCGA-76-4929	0.545205	1	132.1505	47.63228	72.17132	59.83373	4.660162	1.578536	high
TCGA-06-0210	0.558904	1	132.6637	23.60292	30.64785	36.9697	10.20039	0.867921	low
TCGA-32-2638	0.578082	1	138.0039	35.93231	54.23497	31.32749	8.398541	0.906184	low
TCGA-76-4931	0.59726	1	206.52	46.3373	45.81722	44.76383	11.05181	1.260377	high
TCGA-15-0742	0.613699	1	140.2915	51.77297	51.50417	39.23977	7.642791	1.143086	low
TCGA-06-0211	0.632877	1	137.4622	40.34184	37.00743	43.08321	7.17278	1.141582	low
TCGA-16-1045	0.632877	1	189.5629	21.41512	33.77338	35.13166	6.343518	1.012997	low
TCGA-06-0750	0.635616	1	214.1866	67.80955	105.8879	28.75555	5.671292	1.285691	high
TCGA-27-2519	0.635616	1	246.4598	54.09209	75.02524	41.32633	3.477736	1.508975	high
TCGA-28-2513	0.643836	1	92.4272	46.08829	59.67444	31.23411	6.011135	0.927367	low
TCGA-02-2486	0.649315	1	202.8742	51.72237	134.1644	42.58534	9.683138	1.399915	high
TCGA-28-5207	0.660274	1	249.7809	36.48221	56.77898	45.59285	8.330949	1.380562	high
TCGA-26-5139	0.663014	1	142.0489	42.97583	59.73121	31.55857	9.442725	0.938152	low
TCGA-27-1834	0.668493	1	173.8029	40.20974	64.40529	39.56591	7.562747	1.175947	low
TCGA-41-3915	0.70137	1	110.5389	50.78608	65.69816	35.63073	4.583821	1.102399	low
TCGA-06-0219	0.70137	1	284.344	71.72125	116.4953	35.94176	3.115479	1.633877	high
TCGA-14-1034	0.717808	1	78.00486	36.94946	44.68549	69.12016	13.87659	1.365421	high
TCGA-28-5216	0.745205	1	233.103	68.47629	126.0057	43.57916	7.246914	1.592525	high
TCGA-06-0130	0.758904	1	151.6874	59.51141	153.388	37.89631	5.606221	1.370916	high
TCGA-32-1980	0.764384	1	179.2239	34.27197	96.54481	28.55438	23.48885	0.672392	low
TCGA-32-2634	0.772603	1	162.9924	51.91409	74.72735	77.57591	6.695917	1.942323	high
TCGA-27-2523	0.772603	1	306.2665	52.58156	49.13376	49.97735	8.001871	1.637298	high
TCGA-19-5953	0.780822	1	107.9234	52.95517	90.52421	50.55217	11.62783	1.272051	high
TCGA-12-0821	0.783562	1	213.9815	41.63904	49.7821	51.27075	4.013296	1.523024	high
TCGA-06-0743	0.786301	1	132.5178	47.62646	57.33837	20.91613	4.887153	0.83911	low
TCGA-26-5135	0.794521	1	97.98138	51.72713	38.20319	28.82615	11.2631	0.779261	low
TCGA-06-0745	0.810959	1	200.6202	70.09513	73.81489	34.8811	3.279742	1.385898	high
TCGA-19-2629	0.816438	1	149.4207	47.73915	59.70498	57.72573	5.361791	1.538915	high
TCGA-06-0649	0.821918	1	184.1714	42.66877	55.02432	26.83747	3.84453	1.036828	low
TCGA-19-2625	0.835616	1	168.2398	42.77317	56.27156	27.66384	4.121188	1.019349	low
TCGA-14-1823	0.841096	1	244.1291	57.43299	142.4175	42.67542	2.630909	1.663639	high
TCGA-14-0817	0.876712	1	292.8486	82.6027	139.8963	46.5586	2.909204	1.935509	high
TCGA-06-0125	0.882192	1	98.89503	26.41783	54.53219	34.74653	7.94453	0.861279	low
TCGA-12-3653	0.89589	1	150.4582	26.95858	15.78032	44.80021	3.654312	1.174116	low
TCGA-06-5859	0.89589	1	184.9683	39.76688	65.82692	47.17211	6.482991	1.358275	high
TCGA-27-1835	0.89863	1	199.1631	40.6902	57.34481	29.29569	4.377708	1.092263	low
TCGA-16-0846	0.90137	1	194.5448	39.89706	53.27018	30.62852	12.18135	0.936065	low
TCGA-06-2557	0.936986	1	202.47	28.04383	47.36417	47.15006	9.956309	1.233923	high
TCGA-06-5417	0.947945	1	153.9124	48.00988	39.71992	73.74442	4.761712	1.824675	high
TCGA-06-5416	0.950685	1	221.3037	63.22576	139.8653	46.6906	3.720026	1.6967	high
TCGA-14-1825	0.961644	1	256.05	58.68413	56.40678	56.05472	3.89726	1.782033	high
TCGA-28-1753	0.980822	1	171.5687	40.83743	52.40134	40.02558	7.762524	1.161219	low
TCGA-41-2571	0.986301	1	157.2702	51.18373	155.181	31.91235	10.95407	1.122988	low
TCGA-06-5414	1.019178	1	110.792	36.88267	27.16114	37.16333	8.885071	0.917248	low
TCGA-27-2526	1.049315	1	464.1159	74.75511	96.82345	29.17577	2.742156	1.832725	high
TCGA-12-0619	1.054795	1	145.8938	39.38512	88.58783	50.39442	13.92942	1.222928	high
TCGA-06-0178	1.057534	1	204.8925	67.6383	53.07445	48.87994	1.934098	1.635517	high
TCGA-14-0736	1.109589	1	315.0677	49.76625	59.79084	30.09368	4.001996	1.374607	high
TCGA-28-5220	1.136986	1	212.9171	36.93462	48.78358	36.7928	3.636213	1.239505	high
TCGA-06-2569	1.156164	1	60.74164	96.66699	89.24749	60.97093	14.49019	1.524882	high
TCGA-14-1402	1.164384	1	219.5947	72.44406	101.2611	41.37018	3.773344	1.581608	high
TCGA-06-5858	1.183562	1	159.7686	36.62517	58.3591	42.46264	9.309692	1.140723	low
TCGA-06-0132	1.183562	1	180.6886	32.31339	47.41941	28.33365	11.96218	0.827996	low
TCGA-14-0787	1.194521	1	220.918	61.67123	73.42849	40.61549	8.502973	1.378601	high
TCGA-06-0157	1.2	1	123.3385	38.17033	24.76579	36.90867	7.431699	0.968431	low
TCGA-06-2559	1.208219	1	79.45879	38.1274	43.24852	51.973	9.931244	1.139391	low
TCGA-06-5856	1.227397	1	260.9341	43.97517	64.35601	38.66656	5.556186	1.379074	high
TCGA-28-5213	1.238356	1	270.915	70.95007	98.37467	37.46188	3.348006	1.601515	high
TCGA-06-0747	1.243836	1	97.50105	33.58041	62.71473	37.14885	7.311408	0.962514	low
TCGA-06-0141	1.252055	1	223.9854	32.98229	65.95908	23.28548	6.383053	0.961812	low
TCGA-27-1832	1.287671	1	117.9798	58.61661	96.97399	37.94333	4.695171	1.24039	high
TCGA-06-0190	1.320548	1	108.3405	50.84246	60.0325	44.06968	8.899403	1.155102	low
TCGA-27-2521	1.328767	1	113.5622	37.93889	51.4531	46.81287	6.922209	1.181307	low
TCGA-02-0055	1.331507	1	138.8048	60.89849	135.3893	46.01912	7.063739	1.445635	high
TCGA-06-0645	1.331507	1	120.4561	47.20002	73.70598	31.70792	8.968882	0.952258	low
TCGA-32-2615	1.350685	1	142.1348	39.10331	76.82889	27.48486	7.314247	0.91483	low
TCGA-06-2570	1.476712	1	147.559	38.70198	38.93062	40.18183	13.41704	0.972097	low
TCGA-28-2514	1.476712	1	118.3961	31.32721	50.78901	39.01003	8.928685	0.97272	low
TCGA-06-5410	1.482192	1	170.8315	52.32214	112.1809	34.79714	12.64312	1.106918	low
TCGA-19-2624	1.49589	1	80.24813	47.48547	56.81296	43.83505	9.113853	1.073872	low
TCGA-76-4932	1.526027	1	239.3557	43.62041	33.84148	45.3495	11.57993	1.289463	high
TCGA-06-0168	1.608219	1	188.0406	44.68316	67.77554	39.29435	8.620589	1.201609	high
TCGA-06-0749	1.610959	1	189.8503	47.63546	70.09753	24.24069	9.745327	0.923306	low
TCGA-15-1444	1.630137	1	113.1966	27.89745	31.10326	34.82031	9.825054	0.821914	low
TCGA-06-0156	1.632877	1	125.6869	45.73678	95.20251	38.09578	5.089312	1.184642	low
TCGA-76-4926	1.652055	1	192.2907	41.9236	51.36432	38.44541	10.7455	1.111927	low
TCGA-02-0047	1.715068	1	95.07924	28.32149	35.14417	30.47295	11.08676	0.690831	low
TCGA-32-2632	1.747945	1	184.9785	49.78746	51.74636	31.69697	4.89668	1.134779	low
TCGA-76-4925	1.810959	1	113.1072	44.81658	79.81849	51.86881	10.20497	1.280223	high
TCGA-06-2563	1.824658	1	124.4889	36.99696	49.49005	43.59746	7.585784	1.12118	low
TCGA-06-1804	1.931507	1	76.4628	23.87607	29.41444	41.252	15.28797	0.73696	low
TCGA-14-0781	1.931507	1	131.6691	45.25588	63.33813	25.33492	10.76343	0.793919	low
TCGA-27-2528	2.013699	1	143.5559	44.53424	62.30331	41.09812	7.532667	1.166779	low
TCGA-19-0957	2.019178	1	143.9576	27.56614	45.95651	36.58202	21.5179	0.68809	low
TCGA-06-2562	2.046575	1	129.9727	58.72473	66.34029	29.68813	16.31588	0.824286	low
TCGA-12-3652	2.191781	1	154.9114	55.66078	34.60847	39.01928	4.823193	1.217955	high
TCGA-12-3650	2.221918	1	135.1143	56.73686	41.25431	46.71792	4.260132	1.349508	high
TCGA-28-5218	2.232877	1	79.73408	53.4883	60.81488	47.41537	4.404275	1.271265	high
TCGA-28-5215	2.232877	1	240.3952	47.04672	59.00184	45.95201	5.647181	1.479769	high
TCGA-28-1747	2.391781	1	223.7125	35.01188	44.93107	38.69473	9.304269	1.161332	low
TCGA-06-0152	2.50411	1	93.16275	40.79991	67.62545	39.73804	11.15678	0.964041	low
TCGA-06-0184	2.909589	1	163.4427	51.14757	75.06089	39.00222	5.224	1.263657	high
TCGA-12-0616	2.909589	1	153.6941	65.8019	98.95527	54.67056	4.35653	1.656971	high
TCGA-06-0882	3.131507	1	198.8553	36.31877	54.06141	32.75498	12.71088	0.955934	low
TCGA-06-0238	3.153425	1	259.5296	66.77627	98.84294	43.38579	6.457049	1.605199	high
TCGA-06-2564	3.180822	1	133.3313	31.50431	59.00513	39.06053	8.061897	1.032185	low
TCGA-19-2619	3.378082	1	90.07406	25.51777	36.80807	33.21863	7.64932	0.79246	low
TCGA-06-0171	3.668493	1	107.1371	25.02038	45.58779	30.72048	10.36021	0.732333	low
TCGA-41-4097	3.926027	1	121.8796	31.77569	47.96256	27.57082	10.88021	0.726831	low
TCGA-32-1982	3.994521	1	123.0658	44.00258	53.11485	30.63144	6.387371	0.944915	low
TCGA-26-1442	4.432877	1	23.80587	24.4485	41.75758	30.0172	16.11723	0.438371	low
TCGA-06-0187	4.742466	1	239.9417	33.9304	63.53612	32.71935	10.11701	1.087276	low
TCGA-26-5132	5.443836	1	140.59	36.82666	95.00636	49.88235	11.4274	1.253129	high
TCGA-41-2572	8.331507	1	136.0025	32.68664	35.63043	27.07419	6.190418	0.82713	low

© Annals of Translational Medicine. All rights reserved.

Table S4 The result is validated on the GEO datasets (GSE83300)

id	futime	fustat	PRDX1	SEC61B	TXN	XRCC5	BCL2L2	riskScore	risk
GSM2198606	1.421096	1	158.5011	47.44586	70.23023	43.02052	6.151619	1.283959	high
GSM2198621	1.089041	1	158.6632	45.31044	67.63565	40.81352	8.719337	1.176295	low
GSM2198638	1.248493	1	159.0652	46.06398	68.78135	43.68051	8.227831	1.245121	high
GSM2198650	0.810411	1	162.2663	47.31064	71.20021	43.43334	10.75034	1.203611	high
GSM2198635	1.431781	1	160.879	43.46473	70.48607	36.49387	14.22017	0.98221	low
GSM2198625	0.961644	1	161.0721	44.92775	70.02774	36.63123	13.75186	1.00116	low
GSM2198647	0.507945	1	162.0038	48.29496	70.6601	41.88264	4.096471	1.316984	high
GSM2198631	1.132603	1	160.2842	46.93892	70.90604	41.20961	5.462799	1.266941	high
GSM2198649	1.596986	1	158.1686	47.78961	71.58481	43.75235	5.911007	1.305436	high
GSM2198640	0.756986	0	161.1215	43.29883	70.36428	35.91489	15.40181	0.946496	low
GSM2198628	0.656712	1	160.5564	45.56183	69.81504	43.22226	9.63876	1.209254	high
GSM2198626	2.232329	1	161.9134	47.65329	72.82851	42.19876	10.42718	1.191133	high
GSM2198634	1.44	1	161.1763	46.13161	71.83742	41.25074	8.545298	1.20275	high
GSM2198623	0.877808	1	160.6083	46.54484	66.71349	43.80434	9.330568	1.226516	high
GSM2198617	3.523562	0	162.1622	44.61726	66.11918	41.6441	2.917961	1.312973	high
GSM2198619	2.870137	0	162.0734	44.65216	70.37382	36.59659	13.43372	1.00817	low
GSM2198622	0.535068	1	164.6226	44.88713	67.61092	41.70163	8.282754	1.210514	high
GSM2198610	1.116164	1	161.8135	43.3809	68.12242	40.0803	15.26726	1.023949	low
GSM2198632	2.134521	0	159.6826	43.17884	68.49758	40.88172	8.584207	1.173276	low
GSM2198636	1.296986	0	161.6886	45.27234	66.87629	39.81109	5.099265	1.237431	high
GSM2198624	2.767397	1	158.7431	44.7161	66.01263	42.6376	5.592995	1.2696	high
GSM2198633	1.578082	1	160.4605	44.80295	68.14713	41.38813	3.651932	1.293815	high
GSM2198608	1.029863	1	158.9377	46.65563	69.46389	42.53322	9.629252	1.198582	high
GSM2198645	1.60274	1	158.2679	44.48455	67.56667	39.879	8.103859	1.167172	low
GSM2198616	1.496712	1	161.0128	48.33633	70.8353	41.24672	9.134263	1.199222	high
GSM2198613	2.599726	0	161.6886	47.2491	69.88271	40.11478	7.669721	1.203527	high
GSM2198651	1.762192	0	160.6083	47.52619	69.13951	41.60163	7.064177	1.241606	high
GSM2198627	1.807397	0	160.4605	46.42049	69.98005	42.1178	9.307213	1.2001	high
GSM2198629	1.070137	1	160.474	45.08372	69.32687	39.7867	11.17931	1.111084	low
GSM2198612	3.802192	1	159.6018	47.04356	72.87525	45.81499	4.9017	1.365196	high
GSM2198620	1.343014	1	161.8791	46.79922	67.10441	39.72549	5.935078	1.226505	high
GSM2198648	0.908219	1	162.2194	47.8651	71.32424	41.72115	10.87167	1.172471	low
GSM2198639	3.488219	0	158.7135	43.76471	68.71442	36.12018	13.30507	0.989212	low
GSM2198641	1.52137	1	159.1846	47.14843	69.2003	39.60023	5.552775	1.232018	high
GSM2198655	0.77589	1	158.8376	47.70972	69.35851	41.88617	6.496708	1.256579	high
GSM2198630	2.942466	1	162.7697	45.57526	67.29524	40.61352	4.543426	1.267757	high
GSM2198614	0.367397	1	159.4361	45.881	71.25549	39.31793	8.740576	1.158004	low
GSM2198637	0.759452	1	160.773	46.15948	68.38086	42.90547	6.849474	1.262572	high
GSM2198611	2.1	1	160.9429	47.59477	73.38612	42.10188	8.165656	1.235151	high
GSM2198607	3.510411	0	161.8217	44.73034	70.06024	37.67286	12.52959	1.04614	low
GSM2198653	0.913151	1	160.2465	43.58849	70.04769	38.88511	14.75297	1.013733	low
GSM2198609	0.683836	1	161.0047	47.56048	70.99878	42.42731	7.386254	1.253707	high
GSM2198644	1.483562	1	157.1923	46.75535	70.47631	39.39552	8.940903	1.154179	low
GSM2198652	2.610411	1	158.0662	43.4521	69.93959	37.25537	15.00604	0.973787	low
GSM2198615	1.367671	1	160.5731	43.20611	69.4625	37.36482	15.62775	0.965573	low
GSM2198646	1.875616	0	161.0646	45.08518	68.30957	40.04181	9.239542	1.155666	low
GSM2198643	0.980548	1	160.9683	45.93237	69.55838	42.18097	7.952068	1.227394	high
GSM2198642	1.527123	1	153.4301	46.47485	69.59679	38.71802	10.58431	1.098029	low
GSM2198654	1.043014	1	162.6299	47.85886	68.13601	42.66464	7.174759	1.262597	high
GSM2198618	1.034795	1	158.1369	47.51073	68.69376	45.02126	7.87105	1.282224	high

© Annals of Translational Medicine. All rights reserved.
http://dx.doi.org/10.21037/atm-21-1986